

**SINGLE-STAGE, NORTHEAST-DIRECTED THRUSTING ON THE
LARAMIDE BEARTOOTH FAULT**

Timothy R. Nielsen

A thesis submitted to the faculty of the University of North Carolina at Chapel Hill in partial fulfillment of the requirements for the degree of Master of Science in the Department of Geological Sciences.

Chapel Hill
2009

Approved by:

Dr. Kevin Stewart

Dr. Louis Bartek

Dr. Jose Rial

ABSTRACT

TIMOTHY R. NIELSEN: Single-stage, northeast-directed thrusting on the
Laramide Beartooth fault
(Under the direction of Dr. Kevin Stewart)

This study focuses on the synkinematic sediments along the Beartooth thrust fault in order to assess both the Laramide paleostress history of the Beartooth uplift, and how far the Bighorn Basin's syn-orogenic deposits have been overridden. The sediments shed into the basin by the ascending Beartooth block were folded and overridden by the Beartooth thrust. In the vicinity of Red Lodge, MT, the Paleocene/Eocene sediments were overthrust 4-7 km, based on truncated alluvial fans. These sediments contain a population of two orthogonal systematic joint sets. The older of the two strikes NE-SW and the younger abutting set strikes NW-SE. These uncomplicated footwall joint-sets reflect the stress field of single-stage, northeast-directed thrusting on the Beartooth fault, and suggest that the stress field record did not include a purely E-W second stage of uplift, as proposed by previous researchers.

PREFACE

There are challenges in life, some from circumstance and others self-imposed. Graduate school was for me a mixture of these two, and without my family and friends I would have met none, yielded much, and learned nothing.

TABLE OF CONTENTS

Chapter

1.0	INTRODUCTION	1
2.0	GEOLOGIC SETTING	4
	The Bighorn Basin	4
	Basement Rocks.....	5
	Paleozoic and Mesozoic Stratigraphy	5
	Paleocene/Eocene Stratigraphy	7
	Beartooth Thrust Fault	8
	Bighorn Basin Axis.....	9
3.0	TECTONIC JOINTS	12
	Correlations between joint trends and principal stress axes ..	13
	Joint Surface Morphology	14
	Timing of joint formation.....	14
	Geometrical relationships between joints.....	15
	Nonsystematic fractures	16
	Formation Mechanisms of Front-Normal JT ₂ Joints	17

4.0	DISPLACEMENT ON THE BEARTOOTH THRUST	20
	Amount since the fan material was deposited.....	23
	Total amount of thrusting	23
5.0	DISCUSSION	25
	Tectonic Inheritance	26
6.0	SUMMARY	28
	APPENDIX A, FIGURES	29
	Figure 1, Basement Fault Map, Central Rocky Mountain Foreland.....	30
	Figure 2,Geologic Map	31
	Figure 3a, 3b, 3c, 3d, Schematic stress orientations	32
	Figure 4, Lower hemisphere plot	34
	Figure 5, Interfingering fan facies	35
	Figure 6 Cross section A-A'	36
	APPENDIX B, TABLES	37
	Data Tables	38
	REFERENCES	42

List of Abbreviations and Symbols

JT_1	Joint population one
JT_2	Joint population two
km	kilometer
m	meter
n	number of
=	equals
>	greater than
σ_1	sigma one, greatest compressive stress
σ_2	sigma two, intermediate stress
σ_3	sigma three, least compressive stress
°	degrees

CHAPTER 1

INTRODUCTION

The Beartooth Mountains and adjacent Bighorn Basin are major Laramide structures of the middle Rocky Mountain foreland province (Figure 1, Appendix A). The diverse structural trends of Laramide-aged faults and folds have previously been attributed to different episodes of shortening. The Laramide stress history responsible for the current arrangement of the Beartooth Mountains and Bighorn Basin, and the amount the basin has been overridden by the Beartooth thrust have been the subject of debate. Specific to this study is the apparently wrenched axis of the Bighorn basin. It changes in orientation at the southern terminus of the Beartooth Mountains as it intersects the Beartooth thrust. Wise (2000) attributed this to two stages of uplift; northeast-directed thrusting followed by east-west. This study seeks to provide estimates of both the magnitude, and direction of thrusting on the Beartooth Fault. Both the paleostress record and the amount of overthrusting can be estimated by studying exposures of the deformed sediments shed during uplift along the margins of the basin.

The Bighorn Basin syncline was created by horizontally directed Laramide shortening. As the fold deepened, sediments from adjacent uplifts formed synkinematic deposits, including the Paleocene Fort Union Formation, which is

integral to this study. The central and southern segments of the Bighorn Basin axis trend northwest-southeast which is consistent with orthogonal northeast-southwest shortening (Blackstone, 1986). The basin axis appears to bend abruptly northward with the southeastern corner of the Beartooth uplift. Wise (2000) concluded that the bend in the axis of the Bighorn Basin was caused by a regional shift from northeast to east-directed thrusting, maintaining the orthogonal relationship between tectonic shortening and folds axes. Recent physical analog studies demonstrate that differently oriented basins and arches do not require separate episodes of deformation with different shortening directions (Bump, 2000). Similarly, differing Laramide-aged structural trends have recently been shown to be due to reactivation of pre-existing structures, and not from multiple Laramide shortening directions (Larson et al., 2007).

To test the two-stage shortening model this study focuses on outcrops in the northwestern part of the basin, along the southeastern edge of the Beartooth uplift, in proximity to the Beartooth thrust fault. If northeast-directed thrusting was followed by a shift to east-directed thrusting, deformation features in these rocks, such as joints, should record this change. Joints are a particularly useful structure because they form in response to small strains and therefore can be used to infer paleostress orientations (Hancock, 1994).

Synkinematic alluvial fan deposits of the Paleocene Fort Union Formation have been folded and overridden by the Beartooth Mountain hanging wall block (Decelles et al., 1991a,b). The amount of overthrusting has been estimated by others using several methods. These include correlations of bore well data sets

(Blackstone, 1986), basic measurements of map-view apparent offsets of prominent limestone palisades, and kinematic unroofing history studies (Decelles et al., 1991a,b). Complications arise with each technique. For example, the apparent map-view offsets measured along the Willow Creek and Maurice 'tear' faults are invalid indicators of the magnitude of thrusting on the Beartooth Fault for a number of reasons. Namely, the faults have since been shown to be in fact high-angle normal faults (Bartholomew, Wise and Stewart, 2004). Other researchers have interpreted bore well data to produce cross section which show an estimated amount of thrusting on the fault. These estimates and cross-sections explain the data, but use an assumed slip vector for that displacement. Cross-sections do not show maximum displacement unless they are drafted parallel with the slip vector. In these previous estimates, this slip vector, which is synonymous with the local shortening direction of the Laramide orogeny, is approximated. The kinematic history determined through a combination of synorogenic conglomerate clast composition/provenance and internal stratal architecture (DeCelles et.al.,1991) provides valuable points. Namely, that considerable foreland uplift was accomplished by fault propagation folding before the breakout of the Beartooth thrust fault. Problems remain, however, in that the kinematic models used in the study were based upon stepwise retro deformation of balanced cross-sections using an outdated 30 degree dip for the Beartooth Thrust Fault, and purely east-west shortening.

CHAPTER 2

GEOLOGIC SETTING

The Laramide orogeny approximately Late Cretaceous through Early Tertiary, is differentiated from the contemporaneous Sevier orogeny on the basis of structural styles. Laramide structures are characterized by basement-block uplifts, in which the major detachments originate in the crystalline basement below the sedimentary cover, as opposed to shallower detachments associated with the Sevier.

Laramide basement-involved uplifts, from north to south, include the Beartooth Mountains, Bighorn Mountains, the Owl Creek range, Wind River and Laramie ranges, Uinta Mountains and the southerly Front Range. Basins adjacent to and between the major uplifts include the Bighorn, Powder River, Green River, Uinta, Piceance, Denver, and the San Juan Basins. Laramide structures within the Colorado plateau include the East Kaibab Monocline, the San Rafael Swell, Circle Cliffs, Monument Uplift, Defiance Uplift, and White River Uplift, respectively (Miller et al., 1992).

The Bighorn Basin

The Beartooth Mountains and Bighorn Basin lie in the middle Rocky Mountain foreland province. The Bighorn Basin syncline is bordered by Laramide fault-bounded uplifts; the Beartooth Mountains on the western limb and the Bighorn Mountains on the east. It is an asymmetric tectonic basin, with a steeper western limb due to the greater shortening along the Beartooth thrust. The

Absaroka and Owl Creek mountains lie to the south of the basin, and the northernmost portion of the basin is open and not bounded by uplifts. Instead, it gives way to the Nye-Bowler lineament, which is a zone of northwest-southeast trending predominately left-lateral faults and associated folds. Structural relief between the basin and adjacent Beartooth uplift is about 9 km (Blackstone, 1986).

Basement rocks

The basement rocks of the Bighorn Basin and Beartooth uplift are Precambrian (1.2-2.4 Ga) crystalline rocks that range in composition from granitic gneiss to ultramafic rocks. The Bighorn Basin's syncline axis is covered with as much as 7,000 meters of Paleozoic, Mesozoic, and lower Cenozoic sedimentary rocks (Foote et al., 1961, Blackstone, 1986, DeCelles et al., 1991a,b).

Paleozoic and Mesozoic stratigraphy

Basal Cambrian rocks are represented by the thin (0-20 m thick) transgressive shoreline Flathead Sandstone. It is a light-reddish, medium-to-coarse-grained sandstone overlain by the Wolsey Shale (20-70 m thick), which consists of green and gray marine shales. The Meagher Limestone (10-30 m thick) consists of thinly-bedded shallow marine limestone with shale interbeds. The Park Shale (100-160 m thick) consists of green marine shale containing lenses of thin limestone. The upper 10-15 meters of the Park Shale is composed of the distinctive Edgewise conglomerates, which are characterized by randomly oriented shale rip-up clasts. This unit is overlain by the resistant Maurice Formation (30-50 m thick), a mottled, thickly bedded, shallow-marine limestone, of which some beds are composed of oolitic sands. The Snowy Range Formation

(75-100 m thick) overlies the Maurice and consists of greenish-gray shale interbedded with gray dolomites and pebbly conglomerates.

The 100 m thick interbedded Devonian Jefferson Limestone is overlain by the Devonian Bighorn Dolomite (50-120 m thick) which is a massive shallow marine carbonate that forms prominent ridges. Atop these lies the massive shallow marine Mississippian Madison Limestone (200-300 m thick), which is resistant and vuggy. These massive carbonates form the impressive limestone palisades and flatirons in the vicinity of Red Lodge, MT.

The distinctive redbeds of the Triassic Chugwater Formation (180-210 m thick) are comprised of red siltstones, shales, and fine-grained sandstone. These are overlain by Jurassic formations which are undivided in this paper. Notable formations, however, include the Gypsum Spring and Sundance Formations (130-150 m thick combined) of middle and late Jurassic age, respectively, as well as the late to early Cretaceous Morrison and Cloverly Formations (170 m thick combined). The Gypsum Spring Formation consists of red and gray shale, fossiliferous limestone, and gypsum. It is overlain by the Sundance Formation, which consists of green and gray shale, greenish-gray, glauconitic, limy sandstone, and thin beds of fossiliferous limestone. The Cloverly Formation includes light gray sandstone, gray variegated shale and a reddish lenticular chert conglomerate top. The Morrison Formation is of late Jurassic age, and composed of dully variegated claystone and gray silty sandstone.

Rocks of the Cretaceous Period are also undivided in this study. Notable Formations include the lower Cretaceous Thermopolis Shale (170 m thick) which is composed of soft black shale interbedded with bentonite beds, the Mowry Shale (135 m thick) which is composed of gray and brown partially siliceous

shale with bentonitic interbeds and abundant fish scales, the Frontier Formation (135 m thick), composed of thick lenticular gray sandstone, gray, brown, and carbonaceous shale, and bentonite. This is overlain by the Cody Shale (550 m thick), which has a lower dark gray thinly bedded marine shale and an upper portion composed of buff sandy shale and thinly laminated buff sandstone (Mesozoic descriptions from Pierce, 1965).

The carbonate and siliciclastic rocks which overlay the crystalline basement of the Beartooths and Bighorn Basin are well exposed in the field area along the edges of the Beartooth uplift. The geomorphology of the steeply dipping weathered sequence above the Beartooth Thrust fault demonstrates the differential weathering characteristics of the strata. The more resistant cliff-forming carbonates are interstratified with less-resistant terrigenous shales, which tend to form saddles and slopes.

Paleocene/Eocene stratigraphy

Uplift of the approximately 60x120 km Beartooth block during the Laramide orogeny was accompanied by synkinematic sedimentation along the northern and eastern margins of the structure. Approximately 3 km of Phanerozoic terrigenous rocks and marine carbonates (Dutcher et al., 1986) were eroded along with rocks from the Precambrian crystalline core of the Beartooth uplift. These synkinematic deposits contain an inverted erosional sequence (Dutcher et al., 1986) reflecting the progressive erosion and unroofing of the Beartooth uplift.

The lower Paleocene Fort Union formation was deposited early during the Bighorn Basin's formation, and consists of sandstones and siltstones with some

minor coals. It is 2500 meters thick in the vicinity of Red Lodge, Montana and has been subdivided into four members (DeCelles et al., 1991a,b): the basal Tullock Member, the Lebo Member, the Tongue River Member, and the Linley Conglomerate.

The Tullock Member consists of fine-grained sandstones, siltstones and shales. It represents an alluvial environment with anastomosing channels (Brown, 1993). The Lebo member conformably overlies the Tullock with a gradational contact of buff Tullock sandstones and shale changing to dark olive-grey shales of the Lebo. Depositional environments for the Lebo Member are small lakes with clastic input from the Beartooth and Bighorn Mountains (Yuretich et al., 1984).

The Tongue River Member overlies the Lebo and consists of up to 800 meters of interbedded fine-to-medium grained sandstones, shales, and minor coal. Depositional environments range from swamps to stream channels (Merin and Lindholm, 1986).

The Linley Conglomerate is a sequence of synorogenic gravels and interbedded overbank deposits reflecting late Paleocene uplift of the Beartooth massif. It has alternatively been referred to as the Beartooth Conglomerate, and was deposited synkinematically with the Beartooth Fault (Decelles et al., 1991a,b). The depositional environment of the Beartooth Conglomerates are established as alluvial fans and braided streams (Flueckinger, 1970; DeCelles et al., 1989, 1991)

Beartooth thrust fault

The Beartooth thrust trends south along the eastern edge of the Beartooth uplift to Clarks Fork Canyon (Figure 2, Appendix A). Motion on this fault during

the Laramide orogeny lifted the Beartooth block and Paleozoic cover. Along its length, the Beartooth fault juxtaposes Precambrian basement against Paleozoic through Eocene sedimentary rocks, and is covered in places by Quaternary alluvium, pediment gravels, and glacial till. The fault trace commonly corresponds to an abrupt break in slope and is covered by float. Good exposures of the fault surface were not observed, nor were there visible slickenlines or other kinematic indicators. The fault has a shallow (20°) dip near Red Lodge, MT, which steepens southward at Clarks Fork Canyon. The shallow dip of the northern portion is evinced by the fault trace along topographic contours, and also well data from the AMOCO Beartooth Number 1 and 1 A sidetrack boreholes (SW1/4, SE1/4, Section 19, T.8 S., R.20 E., Carbon County, Montana) (Wise, 2000). Amoco initiated this exploratory well, advanced from 1986 through 1988 located west of the range front. It passed through 3100 m of basement before encountering the fault zone and underlying Paleozoic and Mesozoic limestones and shales. Dipmeter readings suggest a fault dip of 10-15° (Wise, 2000) for the Beartooth Thrust due west of its exposure at the range front. The variability in fault dip along its length may be reflecting the ramp-flat geometry of the thrust system, with shallow-dipping locales representing exposures of flats, and steeper-dipping locales representing the ramps.

Bighorn Basin axis

The Laramide basement-involved downward flexure of the older Precambrian-Mesozoic units created accommodation for material shed from the ascending edges into an axial drainage system. The basin subsequently has two axes, a structural axis and a depositional axis. The structural axis is covered,

and can be inferred from borehole and seismic data. The exposed depositional axis is defined by dips on sedimentary rocks which are of Laramide age.

Published maps show the central and southern portion of the basin, between Cody and Powell, Wyoming, as having a northwest trending axial trace. This trend is commonly shown to change abruptly to north-south at Clarks Fork Canyon, Wyoming (e.g. GQ-478 by Pierce, W.G., 1965). This bend also coincides with the southern terminus of the Beartooth uplift. The basin contains numerous smaller basement-cored folds, whose axes trend to the northwest (Foote et al., 1961, Blackstone, 1986). These are well-known from their economic status as petroleum hydrocarbon structural traps (e.g. Elk Basin anticline). In addition, a sizable northwest-striking fold involving mostly exposed Cretaceous units resides in the hangingwall in the vicinity of the Montana-Wyoming state line on the western edge of the basin (Line Creek Fold, Wise, 1983, 2000). In this vicinity, more subtle folds within synkinematic conglomerates of the southern Beartooth Mountains trend north-south (Decelles et al., 1991b).

The Bighorn Basin's structural axis involves Precambrian crystalline basement and younger sedimentary cover. It corresponds to the sharpest flexure of the syncline. The structural axis was encountered by the Amoco 1 well, in the form of a recumbent syncline, with an axial surface trending N60W at a depth of 3100 meters (Wise, 2000). The fold involves Precambrian basement, and Paleozoic-Mesozoic sedimentary rocks.

The synkinematic sediments along the edge of the basin form an overlapping clastic wedge. Original dips of the synorogenic sediments were eastward, and were as high as 10° (Decelles et al., 1991), with most of the slope between zero and five degrees. Modern analogs of these original depositional dips rapidly

shallow away from the mountain front, and plot as synclines on lower-hemisphere projections such as stereonet. However, the original depositional dips in the field area are modified and/or enhanced by tectonics, as evinced by progressive interformational angular unconformities (Dutcher et.al., 1986) with proximal dips as high as 50°. Further out into the basin, the dips are more subdued. Because of this, the depositional axis is more variable, as small-scale folding of the sediments has resulted in subtle anticlines and synclines well out into the basin.

CHAPTER 3

TECTONIC JOINTS

The Beartooth thrust fault surface is poorly exposed and the thrust direction must be inferred from the geometry of associated structures. Thrusting direction on the Beartooth fault can be inferred from footwall folds, classically oriented orthogonally to the axes, yet this method is imprecise. It is imprecise because the shallow dip-data used to plot the axes are from sediments which intrinsically have a wide array of original shallow depositional dips. In this case, other paleostress indicators, such as joints, are useful. Joint sets adjacent to the Beartooth thrust fault in the competent sandstone layers of the Paleocene Fort Union formation are common and well exposed along the eastern edge of the Beartooth uplift. A prominent orthogonal set (JT_1 and JT_2) is the focus of this study and I will show that they are tectonic, of Laramide age, and can be used to clarify the kinematic history of the Beartooth uplift.

The significance of tectonic joints has been widely discussed (e.g. Hancock, 1990, 1994, Engelder, 1985). Jointing represents small strains, typically no more than a few percent extension in a direction normal to the joint surfaces. Because of these low strains, it is possible to infer paleostress directions based on the geometry of systematic joint orientations.

Tectonic orthogonal joint systems are initiated by fracturing parallel with tectonic compression (Dunne and North, 1990). Their study found that well-developed orthogonal joint sets were parallel with, and orthogonal to associated orogenic structures.

Correlations between joint trends and principal stress axes

Principal stress axes (σ_1 , σ_2 and σ_3) by definition are mutually orthogonal. They can be thought of as poles to a set of planes, such as the corner formed by a typical room floor and walls. The orientations of joints reflect the stress field in which they formed. For example, vertical joints with random strikes likely form in a stress regime with the greatest compressive stress (σ_1) oriented vertically, and with the lesser stress axes (σ_2 and σ_3) equal to one-another (Figure 3a, Appendix A). More relevant to this study, is the origin of systematic joints. In cases where the lesser stresses are not equal, the intermediate stress (σ_2) has further influence on the failure plane. Following this same example as above, the vertical joints forming parallel with σ_1 would have their strikes controlled by σ_2 (Figure 3b, Appendix A). Because the orientation of joints is controlled by the orientations of the principal stresses, a uniformly oriented, horizontal compressive stress produces regularly oriented joints whose strikes reflect the orientations of the principal stress axes, and their relative magnitudes. Figure 3c, Appendix A) shows the expected orientations of systematic tectonic joints for horizontally-directed maximum compressive stress.

Joint Surface Morphology

Joint surface morphology is important, as it is indicative as to what kind of stresses acted upon the failure plane. Mode 1 (opening mode) joint surfaces are commonly rough and preserve hackle marks and plumose structures. They differ from smoother, striated Mode 2 joints in that they do not display this evidence of shearing caused by oblique stresses. The majority of joints, including the JT₁ and JT₂ set, in the area of study formed as Mode 1. During propagation the crack tip undergoes normal stress (σ_n) and the two joint faces detach at the crack front. The extension direction is therefore perpendicular to the joint faces, and parallel to the least compressive stress (σ_3). Mode I fractures have therefore proven useful for estimating paleostress directions (Hancock, 1994).

Timing of joint formation

Joints are brittle failures which form in response to stresses and can occur at any given time after deposition. To associate a given set of fractures with a specific tectonic event, there must be some evidence to constrain the timing of joint formation. Both maximum and minimum ages have to be established in order to make a reasonable correlation between a joint set, the stress field responsible for its formation, and a specific tectonic event. Techniques to determine the timing of JT₁ and JT₂ joint formation in the field area utilize both stratigraphic and structural data.

Stratigraphically, a maximum age of jointing can be established because the joints are in Paleocene sediments. Since these are the youngest rocks exposed

we cannot rule out the possibility that the joints are younger than Paleocene based solely on stratigraphic data.

Another technique is to place the JT₁ and JT₂ joint formation in a structural context. The bedded rocks of the Fort Union Formation provide key evidence in resolving the ages of the JT₁ and JT₂ fractures. When plotted on a stereonet, the fractures are shown to be perpendicular to bedding (Figure 4, Appendix A). In locations along the range front where the bedding of the sandstone was tilted after deposition, the JT₁ and JT₂ fractures were also tilted with the host rocks. Specifically, when the bedding is retrodeformed, the joints are restored to vertical.

The JT₁ and JT₂ joints are likely associated with the Laramide because they reside in Laramide synkinematic sediments, and have undergone similar deformation.

Geometrical relationships between joints

The northeast (JT₁) joints vary in orientation from N35-65E (n=15) and do not terminate against other fractures. The fracture surface morphology of these joints is most consistent with purely dilatational displacement (Mode 1), and does not exhibit signs of shear motion (Mode 2). Additionally, Mode 2 jointing typically displays conjugate shear pairs, with the acute bisectrix coinciding with the orientation of σ_1 . The sub vertical southeast trending (JT₂) joints show some slight variation in strike (generally N325W), and consistently terminate against

the JT_1 surfaces. As previously mentioned, JT_1 and JT_2 joints form an orthogonal set.

JT_1 joints within sandstones with strongly convoluted bedding as a result of paleoseismic liquefaction had strikes with much more variability. At these locations, the spacing, strike, and dip of the joints were affected by the irregular bedding

Nonsystematic fractures

Two populations of non-tectonic fractures are common in the field area. Polygonal, multisided fractures similar in appearance to mud cracks, and curvilinear slope-parallel fractures. The highest concentrations of these nonsystematic joints are near cliff edges. I interpret these fractures to be the result of physical weathering.

Subvertical joints are common in locations where bedding shows evidence of soft-sediment deformation. The synkinematic sediments of the Fort Union were subjected to episodic seismic events (Ballantyne, 2004) before lithification, as shown by abundant paleoseismites, including fractures that were commonly filled by clastic sediments. The orientation of the clastic dikes was controlled by the direction of the least compressive stress near the earth's surface, which appeared to be controlled by the surface slope of individual alluvial fans. These seismically induced hydraulic fractures therefore cannot be used to infer the direction of the Laramide compressive stress field.

Formation Mechanisms of Front-Normal JT₂ Joints

In tectonic basins such as the Bighorn both tectonic and non-tectonic fracture forming mechanisms can operate. By studying the joint orientations, surface morphology, and the interaction of the fractures, the various joint formation mechanisms can be differentiated. Orthogonal joint sets can form with or without tectonic input, and can form as a result of various non-tectonic processes including gravity-driven overburden changes, volume changes due to compaction, and hydrocarbon development. Overburden stress field changes include increased stress due to continued sedimentation, or a stress inversion, as erosion removes overlying material. Joints striking parallel with and orthogonal to range fronts are attributed to the geometry and evolution of thrust sheets (Turner and Hancock, 1990). Their study in the Spanish Pyrenees determined stretching of the foreland basin sequence above a basement flexural fold was responsible for front-parallel joints, and front-normal joints from loading by overriding thrust sheets. The joint populations of this study are similar, as they are roughly front-normal and front-parallel

For the purposes of this paper, it is enough to say that both the JT₁ and JT₂ joints are Laramide aged, and offer two reasonable formation mechanisms for the JT₂ population. Perhaps somewhat counter intuitively, the JT₂ dilatational Mode 1 features lie orthogonal to Laramide thrusting.

Single stage NE-directed shortening explains the northeast σ_1 parallel (JT₁) joints, and as previously mentioned, allows two models for the formation of the

JT₂ joints. JT₂ joints consistently terminate against the JT₁ joints, and are younger, but still associated with the Laramide stress field. The two models for the formation of the younger JT₂ joints are a) folding-related and b) stress-field relaxation related. Folding-related formation of the younger JT₂ joints matches the data, lying parallel to sub-parallel with fold hinges. An alternate hypothesis is that formation of the JT₂ joints occurred after some relaxation in the Laramide stress field, as unloading or release joints (Tindall and Davis abs, 2002).

The JT₂ joints are arguably associated with folding because of locations where the JT₂ joints have been folded along with bedding. If they resulted from a relaxation of the Laramide stresses, then it requires a resumption of that stress to further deform both the bedding and the JT₂ joints. This implies an episodic relative stress inversion.

This stress inversion is analogous to the joints formed in rising bodies of material, such as granites, during exhumation. However, unlike horizontal delaminations formed in response to a decrease in gravity-driven overburden, vertical unloading joints form in response to the decrease in horizontal Laramide compression. As the material in the basin was under some pressure state, due to vertical gravity-driven overburden, an additional horizontal component was added by the Laramide contraction. When the Laramide orogeny ceased, the thrusting also ceased, and the basin sediments released this pressure. The pressure release caused fractures orthogonal to the release, which reflects a change in the relative magnitudes of the principal stresses. The change was from horizontally-dominated Laramide thrusting, to vertically dominated, gravity-

driven stress. The principal stresses changed with time, in magnitude but not orientation. As a result, the material response was that of an elastic rebound. Overall, this response is a volume expansion, with dilational brittle failures accommodating the change.

To recap, JT_1 (northeast) joints formed first, and are mode 1 features, parallel with the maximum horizontal stress. The JT_2 joints are also Mode 1 fractures, and consistently terminate against the JT_1 features. These younger joints either formed through local folding and stretching of the footwall (Turner and Hancock, 1990), or as are unloading and release joints (Tindall and Davis, 2002).

CHAPTER 4

DISPLACEMENT ON THE BEARTOOTH THRUST

The kinematics of the Beartooth uplift, along with the direction and magnitude of thrusting on the Beartooth detachment, has been the subject of numerous studies (e.g. Blackstone 1986, DeCelles et al.,1991; Wise, 2000). Data from the AMOCO Beartooth Number 1 and 1A sidetrack boreholes (SW1/4, SE1/4, Section 19, T.8 S., R.20 E., Carbon County, Montana), drilled down through hanging wall several kilometers west of the range front, confirmed that the Beartooth thrust fault has a shallow (19°) dip. The borehole penetrated identifiable sedimentary formations beneath the thrust. This information provides valuable constraints on thrust models and subsequent cross sections. Without slip vector information, however, balanced (restorable) cross sections showing maximum displacement must be drawn with the assumption that the slip motion and deformation is parallel with the strike of the cross-section

Clast composition studies have identified different zones within the Paleocene alluvial fans (DeCelles et al.,1991a, b). Using these zones, the initiation of the uplift can be modeled as that of a subdued monocline, with structural relief providing the impetus for erosion (DeCelles et al.,1991a,b). The resulting sedimentary material would lap up on this structure. As progressive uplift of the

Beartooth block ensued during the Laramide the synkinematic sediments were folded, cut, and overridden. There are few estimates of the amount of overthrusting undergone by the synkinematic sediments.

Generally, the fans original morphology can be characterized as concave in cross section, with higher steeper slopes gradually becoming less steep down dip. The size of the clasts making up the fans fine with distance away from the steeper slopes.

In the vicinity of Line Creek Montana, a continuous exposure of sands and gravels follows a modern drainage system down slope to the east (Figure 2, Appendix A). It has been previously mapped as the Linley Conglomerate unconformably overlying the Tongue River member of the Paleocene Fort Union Formation. Field work I conducted reveals otherwise. The interfingering relationship of Linley conglomerates and Tongue River sands (Figure 5, Appendix A), shows that these units are time correlative and that they represent deposition in more proximal (conglomerate) and more distal (sand) parts of a fan complex.

The upper-fan material, which is primarily composed of cobbles, is easily accessed along the road leading into Clarks Fork Canyon. The mid-fan facies is well exposed at Gold Creek, as well as extensive exposures following a modern drainage system in the vicinity of Line Creek. The distal sands of the Tongue River Formation are exposed for several kilometers up and down the range front, but the most notable exposures lie along both sides of the Meeteetsee Trail just south of Red lodge, MT. It is here near both the North and South Fork Creeks

that the bedded sandstones lay in the footwall within meters of the covered Beartooth thrust, and dip westward.

Criteria used to draw the sub-boundaries are based upon outcrop descriptions and characterization. Upper fan facies consists of conglomerates and slide blocks and varies from massive to thick bedding. In the hanging wall near Red Lodge, Mt, the finer-grained matrix of the upper fan facies can also be reddish in locations where the clasts consist primarily of limestone.

The mid-fan facies is characterized by interbedded coarse sands and gravels, with lenses of conglomerate. Bedding structures include cross bedding, clast imbrication with some silt horizons.

Distal fan/braided stream facies is characterized by coarse to fine sands with interbeds and lenses of minor coals. It is commonly cross-bedded and contains asymmetric ripplemarks.

The map patterns of the fan facies (Figure 2, Appendix A) show a system with laterally integrated fans, which form rough belts. The trends of these belts indicate that the upper and mid fan facies are missing, or overridden. The mid-fan facies re-emerges from under the Beartooth block near Red Lodge, MT with the same trend. North of Red Lodge, the Sheep Mountain outcrop falls into the edges of both distal facies, as does a smaller hill just south of the Willow Creek fault. Some of these rocks have been interpreted by previous researchers to be post Laramide. This cannot be the case, however, as the originally horizontal dips have been considerably tilted after deposition to approximately 15 degrees. A measurement of this fan truncation yields approximately 4-7 kilometers of slip

on the Beartooth Thrust (Figure 6, Appendix A). The estimate uses the NW shortening direction vector from the paleostress study by measuring southwest back to the projected facies belts from the corner location shown on Figure 2.

Amount since the fan material was deposited

As previously mentioned, the Fort Union fan sediments have been overridden by 4-7 kilometers. This estimate is based on the cross section (Figure 6, Appendix A) by measuring the distance up the fault ramp from the projected upper fan facies belt to the contact exposed at the surface. The minimum distance (4 km) is the distance from the exposed contact to the interfingering contact with the mid-fan facies, and the maximum estimate (7km) is the distance from the exposed contact to the upper extent of the fan facies.

Total amount of thrusting

By placing the overridden fans in the kinematic sequence of the uplift, it appears considerable shortening preceded the breakout of the Beartooth fault. Evidence of this is the onlapping relationship, or angular unconformity, of the upper fan facies directly on the once-horizontal Madison limestone at the corner near Red Lodge. The limestone, conglomerate, and the contact now dip steeply, tilted to a sub-vertical orientation. This implies that the uplift was initiated by folding, followed by erosion of approximately 2500 meters of section, and deposition of the featured conglomerate and alluvial fans. This fan system was further deformed and tilted prior to the eventual breakout of the Beartooth thrust.

When the thrust fault propagated through the lower synkinematic sequence it provided further topographic relief and subsequent erosion and deposition. The Beartooth Conglomerate is thought to be of the same age as the thrust fault (Decelles et al., 1991a,b) however; the featured outcrop of reddish upper-fan facies in the hanging wall is more likely older than the Beartooth thrust.

CHAPTER 5

DISCUSSION

Earlier researchers assumed a poly-phase basin evolution involving two discrete shortening directions; an early phase of northeast thrusting followed by a phase of east thrusting. Evidence cited is the change in the basin axis. The apparently wrenched axis of the Bighorn basin can also be explained by a single prolonged NE-SW contraction. The northern portion of the basin is where the axis apparently is diverted from NW-SE to N-S. This is also where the Beartooth thrust fault originates. One can argue that differential motion, that is, the northern segment moving towards the NE relative to the southern portion, might explain the apparent wrenching of the Bighorn Basin axis. Slip would thus be accommodated largely on the Beartooth Thrust fault. Evidence of this differential motion is the corresponding amount of structural relief. The vertical component of motion is evinced by the greater relief of the Beartooth Mountains at the Red Lodge corner. Southwards of the Beartooth Thrust fault terminus at Clarks Fork Canyon, the mountains are but a subdued monocline, with the basement rocks still covered by draped Paleozoic strata.

Another possibility is that the axis is not drastically bent, but passes beneath the Beartooth thrust. The deformed onlapping synkinematic material which is now exposed along the southern range front has dips to the east. These eastward-dipping beds would in fact plot as having a north-south axis because the dips shallow away from the range front. As previously discussed, the Bighorn basin has two axes, a basement-involved structural axis and a depositional axis. The hypothesis put forward here is that it is this depositional axis which is

obscuring the structural axis. Without differentiating between these two, the surficial Bighorn basin's axis does indeed appear to be markedly wrenched. Data from the Amoco 1 well supports this arrangement, showing that the axis is positioned beneath the Beartooth block, trending NW-SE, in the form of a recumbent syncline (Wise, 2000).

Tectonic Inheritance

The markedly block-like shape of the Beartooth uplift may be a result of pre-existing weakness. The southeastern edge of this block, near Red Lodge, MT forms a distinct corner. The single-stage NE-directed thrusting of the Beartooth fault resulted in oblique thrusting, with dextral strike slip motion on the southeastern edge of the uplift (Wise, 2000). The northeastern edge underwent more front-normal thrusting, with a sinistral component. The current orientation between the edges of the block and slip motion are not those predicted by NE directed shortening, and are probably a result of tectonic inheritance.

The widespread variability of Laramide structural orientations may reflect the orientations of pre-existing basement weaknesses (Figure 1, Appendix A). The reverse faults responsible for uplift of these structures have been the subject of recent studies concerning tectonic re-activation of faults (Bump, 2003, Larson et al., 2007). Reactivation models of pre-existing crustal weaknesses are largely spurred by variable Laramide fault strikes, with seemingly incongruous orientations between fault-bounded uplifts and flexural folds, such as the Beartooths and the northern Bighorn Basin. Map patterns of Laramide faults are largely N-S and NW-SE, strikes which are congruent with known Pre-Cambrian rifts (Huntoon, 1993, Timmons et al., 2001). Other studies of now-exhumed fault zones show evidence of this reactivation (Mittra and Frost, 1981). The influence

of tectonic inheritance on the orientation of the both the Beartooth fault trace, and the surficial orientation of the Bighorn Basin axis is still unclear, but the simple paleostress record discussed in this study may cast doubt on inferred Laramide shortening directions which are based purely on their large-scale orientations.

Tectonic inheritance may have had influence on the structural style of Laramide uplifts. The basement-involved contractional deformation which characterizes Laramide structures is atypical of most back-arc deformation. Most back-arc fold-and-thrust belts, involve shallower, non-basement involved detachments. Numerous hypotheses have been set forth to explain the anomalous character of the Laramide deformation: Shallow-dipping subduction, analogous to the Andes (Allmendinger, 1986; Jordan and Allmendinger, 1986; Dickenson and Snyder, 1978), subduction of progressively younger, and thus more buoyant, Farallon oceanic plate (Engelbrecht et al., 1984), subduction of unusually thick lithosphere, such as an aseismic ridge (Livaccari et al., 1981, Henderson et al., 1984), and clockwise rotation of the Colorado Plateau (Hamilton, 1981, 1988).

Although it seems likely to the author that the Laramide was driven by low-angle subduction of the Farallon plate, the timing of deformation and the changes in shortening direction in the overriding North American plate are still not well understood. This paleostress study contributes to an increased kinematic understanding of the Laramide orogeny by clarifying the relationship between the Beartooth uplift and northern Bighorn basin.

CHAPTER 6

SUMMARY

The contribution of this fracture study, coupled with the kinematic reconstruction using the restored architecture of the synkinematic alluvial fans, has led to an increased mechanical understanding of the joints, folds and regional tectonic knowledge. Laramide paleostress indicators, such as joint sets and footwall folds, indicate a NE maximum horizontal stress vector (N45E). Measuring back along this single shortening direction, the Fort Union Formation has been overridden approximately 4-7 kilometers. The Bighorn basin is considerably overridden at the Red Lodge corner. It is not appreciably overridden at Clarks Fork Canyon, near the MT/WY state line. I conclude that a single NE-SW shortening direction during the Laramide created the various structures along the range front, and cite the footwall joint set data as evidence that the stress field record did not include a purely E-W second stage as proposed by Wise, 2000.

APPENDIX A, FIGURES

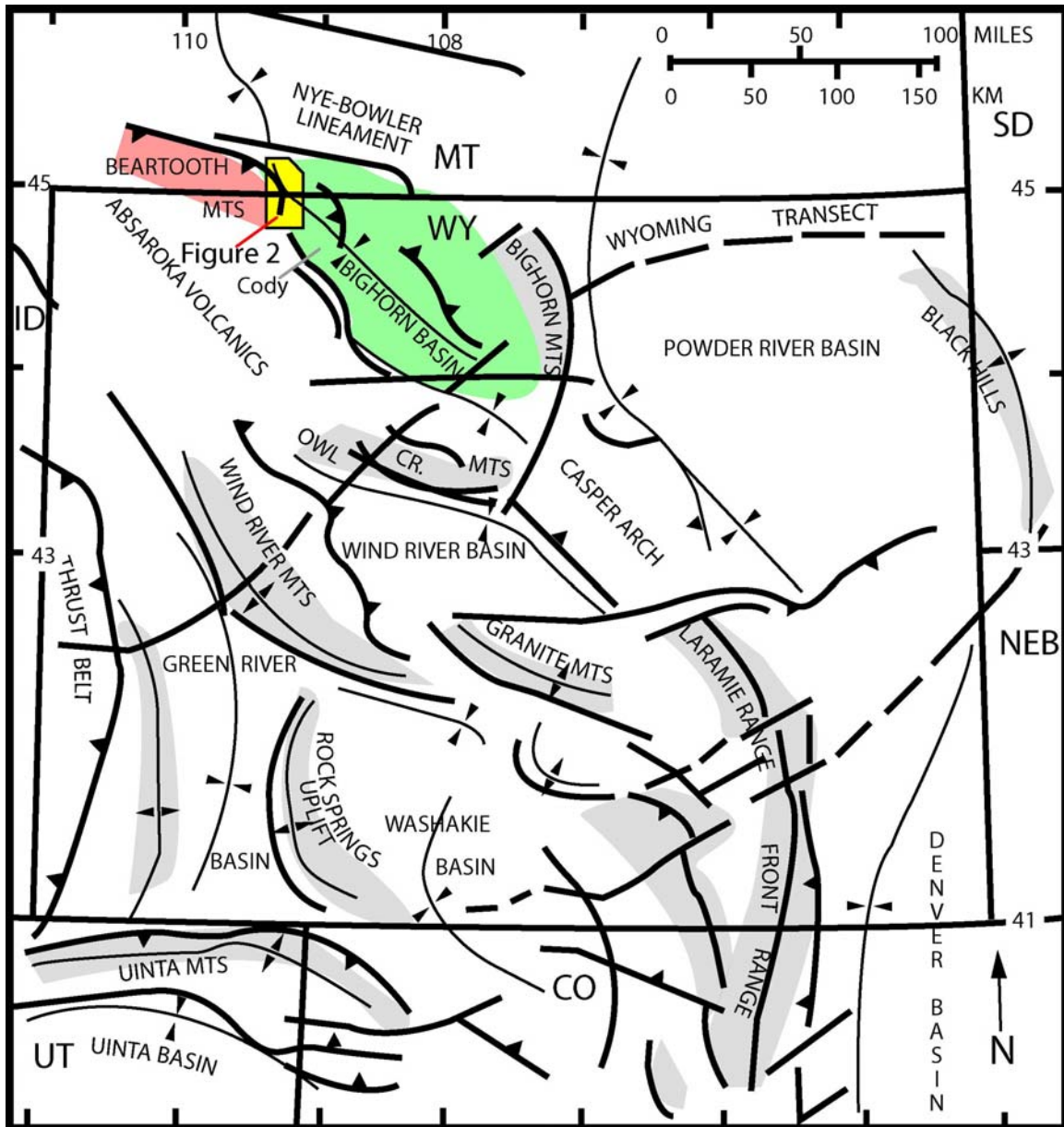
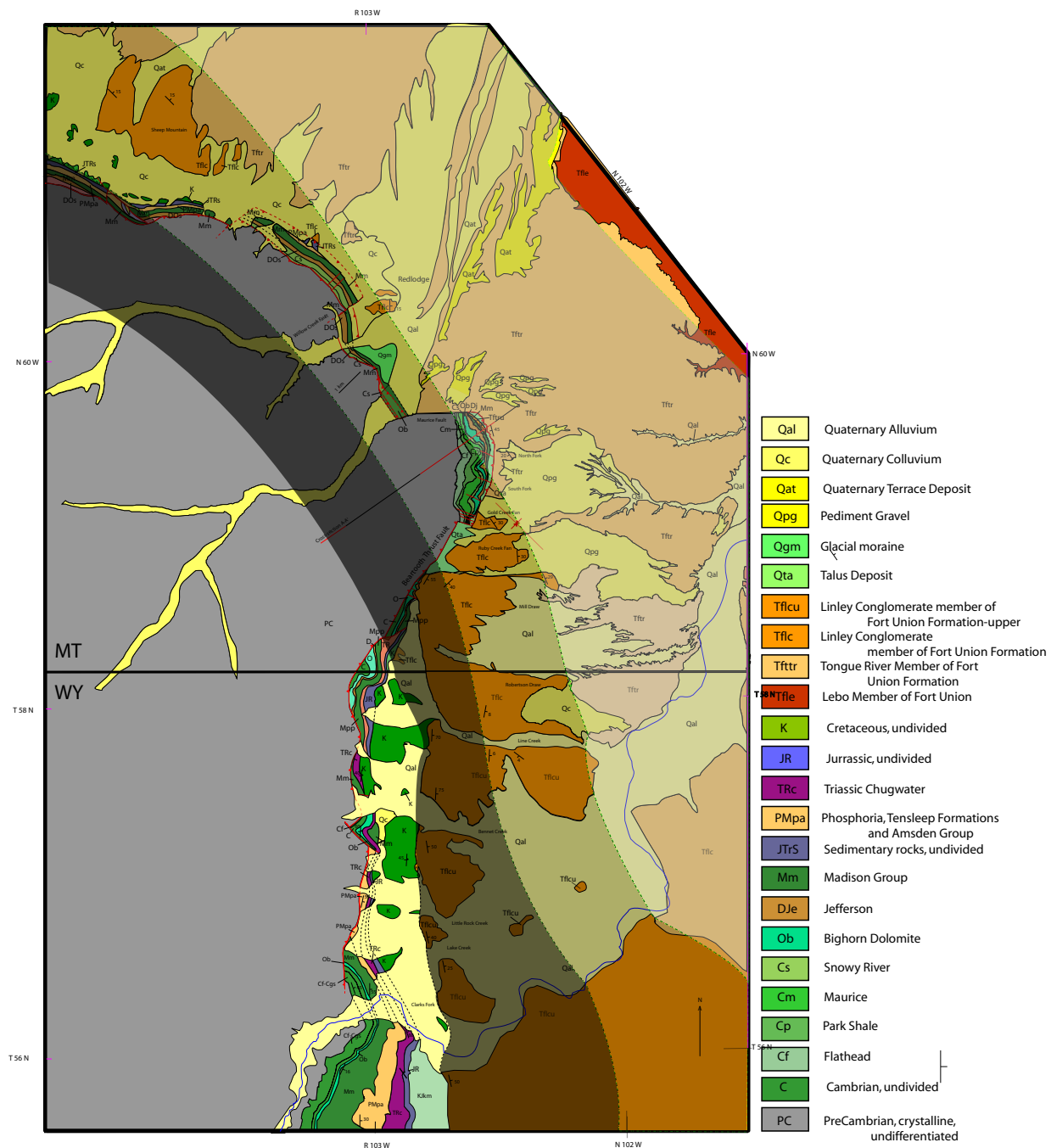
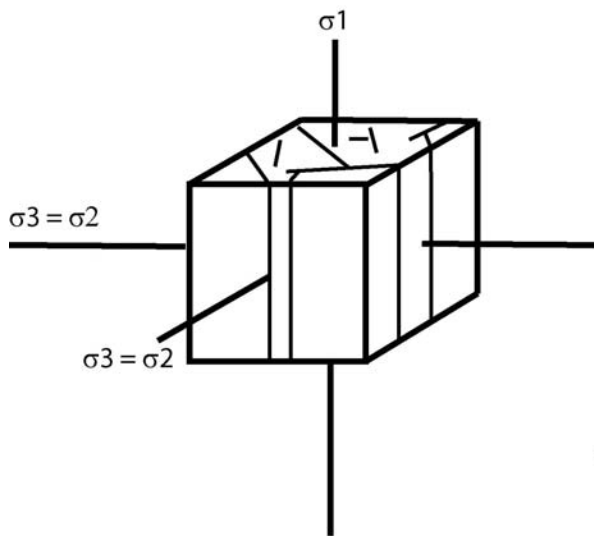


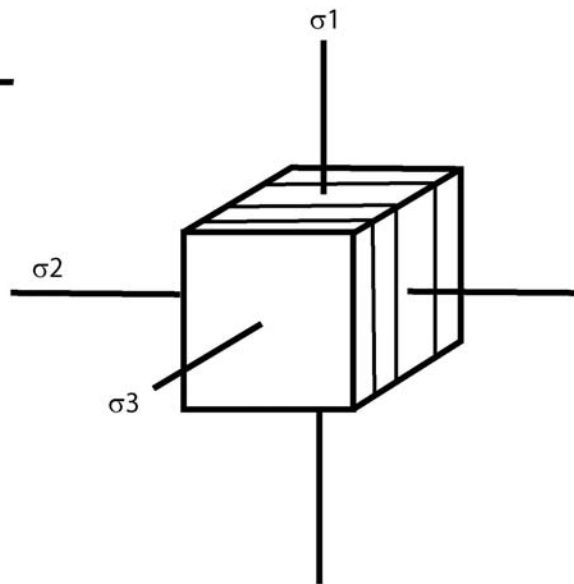
Figure 1: Basement fault map, Central Rocky Mountain Foreland



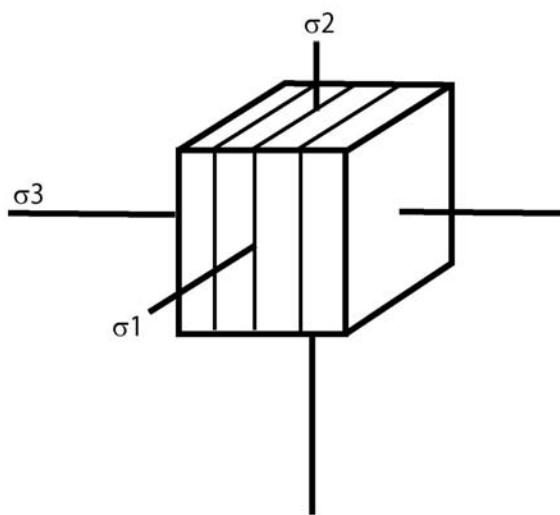
a) $\sigma_1 > \sigma_2 = \sigma_3$



b) $\sigma_1 > \sigma_2 > \sigma_3$



c) $\sigma_1 > \sigma_2 > \sigma_3$



d) $\sigma_1 > \sigma_2 > \sigma_3$

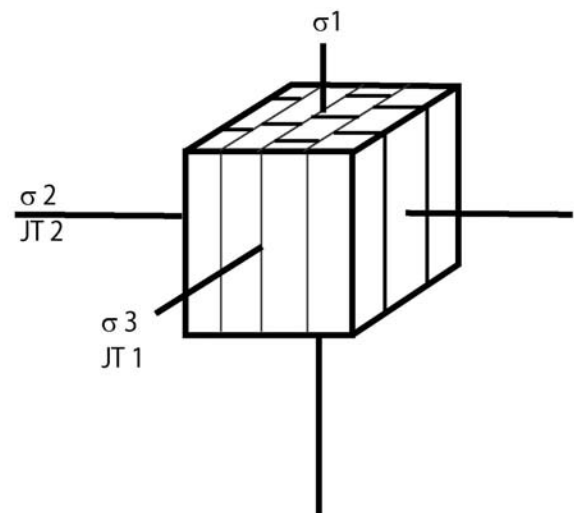


Figure 3: Schematic drawings illustrating expected orientations of joints in different stress regimes. All stresses are compressive. a) Vertical fractures without preferred strikes form where maximum stress (σ_1) is vertical and intermediate (σ_2) and minimum (σ_3) stresses are equal. b) Vertical fractures with parallel strikes form where $\sigma_1 > \sigma_2 > \sigma_3$. Joints form parallel to σ_1 and σ_2 , perpendicular to σ_3 . c) Vertical fractures with parallel strikes can also form when σ_1 is horizontal, such as the JT₁ population. d) Orthogonal set of vertical joints resulting from initial horizontal σ_1 followed by vertical σ_1 . This scenario best explains the orientation of the two joint sets (JT₁ and JT₂) that are present in the Fort Union Formation.

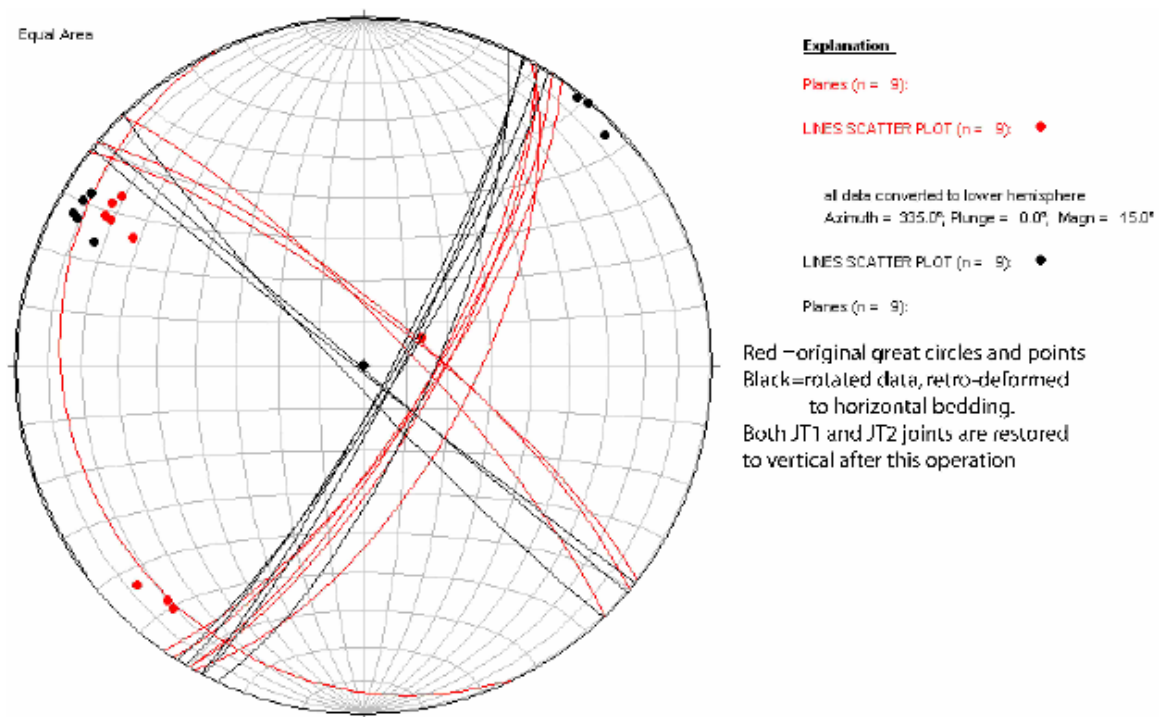


Figure 4: Lower hemisphere plot showing retro deformed bedding, bedding great circles, and restored vertical joint set poles. This is evidence that the joint populations, JT₁ and JT₂, are perpendicular to bedding and have undergone similar deformation as the host rock.



Figure 5: View northeast away from the Beartooth Mountain front near Line Creek, WY. Visible are prominent cliffs of interfingering sands, gravels, and conglomerates. Excellent exposures like this follow modern drainages from the range front, and well out into the Bighorn Basin.

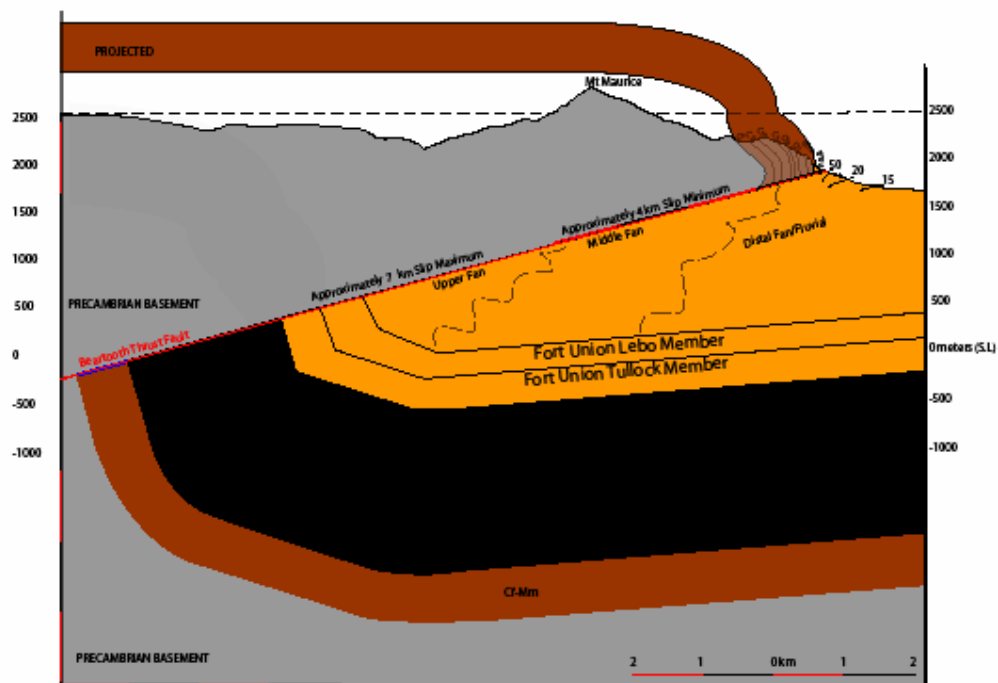


Figure 6: Cross-section drawn parallel with northeast-directed thrusting.

Fan facies belts are projected onto the Beartooth fault, allowing for maximum (7 km) and minimum (4 km) estimates of overthrusting.

APPENDIX B, TABLES

chrono	UTM N	UTM E	strike bed	dip bed	strike joint	dip joint	fault s	fault d	stria
Tol6200501			165	44					
Tol6200502			0	54					
			345	80					
Tol6200503									
Tol6200504									
Tol6220501	639934	4997649	180	35					
Tol6220502	639912	4997604	148	31					
Tol6220503	639928	4997555	158	42					
Tol6220504	639346	4997395	315	68					
Tol6220505	639817	4994338							
Tol6230501	640249	4994456	345	83	185	84			
			356	88					
Tol6230502	640067	4994528							
Tol6230503			335	75			107	71	25
			350	72					
			345	70					
Tol6240501	640316	4994322	206	78			280	65	
							286	66	35
Tol6240502	640278	4994194							
Tol6250501	640769	4991867	320	10					
			285	25					
			280	10					
			275	12					
			220	12					
			195	22					
Tol6250502	640882	4991981	0	15					
			350	12					
			10	12					
			30	13					
Tol6260501	640426	4991865	335	19	116	90			
			335	30	116	85			
			315	20	116	85			
			40	35	110	90			
					117	90			
					135	84			
					130	85			
Tol6260502			0	16	320	83			
					133	85			
					135	85			
Tol6260503	640253	4992132	42	12	130	84			
					143	86			
Tol6260504	639465	4992235							
Tol6260505	639404	4992278	276	68					
			278	74					
			265	70					
			260	70					
			255	65					
			256	64					
			248	44					
			247	33					
			230	35					
			210	27					
Tol6260506							135	68	0
							315	70	50N
Tol6260507			15	60					
			10	68					
Tol6260508							270	56	60E
Tol6280501	639670	4995840	7	56					

chrono	UTM N	UTM E	strike bed	dip bed	strike joint	dip joint	fault s	fault d	stria
Tol6290501			5 210 210	48 81 77			210	77	0
Tol7010501	638171	4988650							
Tol7010502	637247	4989034							
Tol7010503	636996	4989104							
Tol7010504	636825	4989126							
Tol7010505	636998	4989087	300 315 346 270	40 35 40 37	130	84			
Tol7010506	637475	4988817			130	84			
Tol7050501	633828	4935282							
Tol7050502	633939	4984812	215	65					
Tol7050503	633938	4984729	210	65					
Tol7050504	633986	4984569	220	68					
Tol7050505	634026	4984503	215 210	70 70					
Mtm7080501	637271	4989058			90 96 100 275 265 80	81 70 60 70 68 50			
Mtm7080503	637283	4988969	26 25 30	30 25 24					
Mtm7080505	637323	4988820			80 265	77 81			
Mtm7080506	637373	4988817			36 40	26 30			
Mtm7120501	637887	4989476	62 55	30 30					
Mtm7120502	637831	4989499			135 140 72 70 130 130	85 88 60 61 90 80			
Mtm7120503	637795	4989525			130 127 155 160	90 88 82 82			
Mtm7120504	637787	4989537	60 62	30 29	135 138	89 88			
Mtm7130501	637880	4989335	170 165	20 19					
Mtm7130502	637721	4989356	20 300	30 35					
Mtm7130504	637633	4989375	250	16					
Tol7140501	639808	4987349	82 56 75 66	31 23 30 25					
	639524	4987851	0 355	31 30					
Tol7140504	636995	4989074	42	36					
			46	40					

chrono	UTM N	UTM E	strike bed	dip bed	strike joint	dip joint	fault s	fault d	stria
Tol7140506	636695	4989077	30	55			145 245 45	90 80 85	80
Tol7140508	636381	4988775	40 40	78 88					
Tol7140510	636830	4989118	40	45	45	84			
Mtm7160501	636209	4988594	51 50 55	77 77 78	139 133	60 76	315 333	57 42	
Mtm7160502	636071	4988423	48	73			45	85	
Mtm7190501	636209	4988594					345 338 143 338	55 28 75 55	90 90
			50	76	145 147 330 329	88 87 32 33			
Mtm7190504	635990	4988256	33	89	132 313 276 35	82 89 11 32			
Mtm7190507	636056	4988128					327	69	90
Mtm7190510	636122	4988074	45	88					
Tol7200502	640051	4997301	173 185 180 181	32 45 34 40					
Tol7200503	640070	4997102	145 144 151	52 36 55					
Tol7200504	640397	4996805	187 196	39 24					
Tol7200506	640446	4996879	190 196 355 343 333	19 20 13 20 12	303 211 300 30	75 89 80 90			
Tol7200508	640786	4995662	115 125 140 190 165 175	32 15 10 14 11 15	278 293 290 10 345 291 310 272 286	65 61 62 72 78 80 88 82 73			
Tol7230508	641062	4988840	90	10	315	88			

chrono	UTM N	UTM E	strike bed	dip bed	strike joint	dip joint	fault s	fault d	stria
					0	89			
					60	90			
					61	88			
					50	87			
					55	85			
					305	85			
					310	89			
					35	90			
Tol7230509	641068	4988807	315	21	49	83			
			355	34	303	84			
Tol7230510	641079	4988892			123	90			
					110	89			
					50	88			
					125	90			
					40	85			
					25	86			
					55	85			
					160	88			
					120	87			
					70	88			
Tol7240505	641320	4995655	155	15	30	75			
					29	65			
					35	74			
					33	75			
					30	73			
					310	77			
					308	78			
					316	80			
wyo7250504	640294	4983790	0	21	315	87			
			350	21	330	82			
			358	20	325	88			
					315	85			
					245	88			
					240	87			
					237	86			
tol7260506	640993	4991122	185	10	135	77			
			175	8	123	90			
			5	25	144	84			
					230	76			
					229	75			
					134	78			
					124	90			
					221	84			
					245	80			
					235	90			
					60	88			
					305	90			
					310	90			
					295	85			
					305	84			
					303	85			
					70	83			
					60	89			

References

- Ballantyne, H.A., 2004, Understanding the behavior of Laramide paleoseismites in synorogenic deposits: Masters Thesis, UNC-CH
- Bartholomew, M. J., Wise, D. U., & Stewart, K. G., 2004. Structural refinement of the northeastern corner of the Laramide Beartooth uplift, Montana [modified]; Geological Society of America, 2004 annual meeting. Abstracts with Programs - Geological Society of America, 36(5), 268.
- Blackstone, D.L., 1986, Structural Geology—Northwest Margin, Bighorn Basin: Park County, Wyoming and Carbon County, Montana: MGS-YBRA Field Conference Guidebook, p.125-135.
- Brown, J.L., 1993, Sedimentology and Depositional History of the Lower Paleocene Tullock Member of the Fort Union Formation, Powder River Basin, Wyoming And Montana: US Geological Survey Bulletin Report: B 1917-L, pp. L1-L42.
- Bump, A.P., 1999, Strain analysis of the San Rafael swell, Utah, and its implications for the development of Colorado Plateau uplifts. Annual Meeting of the Geological Society of America, Denver, CO, 25-28 Oct 1999. (World Meeting Number 199 945037).
- Bump, A. P. (2003). Reactivation, trishear modeling, and folded basement in Laramide uplifts; implications for the origins of intra-continental faults. GSA Today, 13(3), 4-10.
- DeCelles, P.G., Gray, M.B., Ridgeway, K.D., Cole, R.B., Srivistava, P., Pequera, N., and Pivnik, D.A., 1991a, Kinematic history of a foreland uplift from Paleocene synorogenic conglomerate, Beartooth Range, Wyoming and Montana: Geological Society of America Bulletin, v. 103, no.11, p.1458-475.
- DeCelles, P.G., Gray, M.B., Ridgeway, K.D., Cole, R.B., Pivnik, D.A., Pequera, N., and Srivistava, P., 1991b, Controls on synorogenic alluvial fan architecture, Beartooth conglomerate (Paleocene), Wyoming and Montana: Sedimentology, v. 38, p. 567-590.

Dickinson, W. R., & Snyder, W. S. (1978). Plate tectonics of the Laramide Orogeny; Laramide folding associated with basement block faulting in the western United States. *Memoir - Geological Society of America*, (151), 355-366.

Dickinson, W. R., & Snyder, W. S. (1977). Inferred plate tectonic setting of classic Laramide Orogeny. *Abstracts with Programs - Geological Society of America*, 9(7), 950.

Dickinson, W. R. & Snyder, W. S. 1978. Geometry of subducted slabs related to the San Andreas transform. *Journal of Geology*, **87**, 609–627.

Dunne, W. M., & Hancock, P. L. (1994). Palaeostress analysis of small-scale brittle structures. In P. L. Hancock (Ed.), *Continental deformation* ()Pergamon Press, Tarrytown, NY.

Dutcher, L.A.F., Jobling, J.L., and Dutcher, R.R., 1986, *Stratigraphy, Sedimentology and Structural Geology of Laramide Synorogenic Sediments Marginal to the Beartooth Mountains, Montana and Wyoming: MSG-YBRA Joint Field Conference Guidebook*, p.33-52.

Dutcher, L. A. F., Jobling, J. L., & Dutcher, R. R. (1986). Stratigraphy, sedimentology and structural geology of Laramide synorogenic sediments marginal to the Beartooth mountains, Montana and Wyoming; Geology of the Beartooth uplift and adjacent basins. Paper presented at the Montana Geological Society and Yellowstone Bighorn Research Association Joint Field Conference and Symposium ; Geology of the Beartooth Uplift and Adjacent Basins, MT, United States.

Engebretson, D. C., Cox, A., & Thompson, G. A. (1984). Correlation of plate motions with continental tectonics; Laramide to basin-range; correlation between plate motions and Cordilleran tectonics. *Tectonics*, 3(2), 115-119.
doi:10.1029/TC003i002p00115

Engelder, T. (1985). Loading paths to joint propagation during a tectonic cycle; an example from the appalachian plateau, U.S.A; multiple deformation in ductile and brittle rocks. *Journal of Structural Geology*, 7(3-4), 459-476.

Foose, R. M., Wise, D. U., & Garbarini, G. S. (1961). Structural geology of the Beartooth Mountains, Montana and Wyoming. *Geological Society of America Bulletin*, 72(8), 1143-1172.

Hamilton, W. (1981). Plate-tectonic mechanism of Laramide deformation; Rocky Mountain foreland basement tectonics. *Contributions to Geology*, 19(2), 87-92.

Hamilton, W. B. (1988). Laramide crustal shortening; interaction of the Rocky Mountain foreland and the Cordilleran thrust belt. *Memoir - Geological Society of America*, 171, 27-39.

Henderson, L. J., Gordon, R. G., & Engebretson, D. C. (1984). Mesozoic aseismic ridges on the Farallon plate and southward migration of shallow subduction during the Laramide orogeny; correlation between plate motions and Cordilleran tectonics. *Tectonics*, 3(2), 121-132. doi:10.1029/TC003i002p00121

Huntoon, J. E., & Helsley, C. E. (1993). Tectonic influence on development of the Permian-Triassic interregional unconformity and post-unconformity strata in south-central Utah; AGU 1993 fall meeting. *EOS, Transactions, American Geophysical Union*, 74(43), 577.

Jordan, T. E., & Allmendinger, R. W. (1986). The Sierras Pampeanas of Argentina; a modern analogue of Rocky Mountain Foreland deformation. *American Journal of Science*, 286(10), 737-764.

Larson, S. M., Neely, T. G. & Erslev, E.A., Controls on structural variability in Laramide basement-involved arches, USA. Colorado State University, Department of Geosciences, Fort Collins, CO 80523, smlarson@colostate.edu, (2) Department of Geosciences, Colorado State University, Fort Collins, CO 80523

Livaccari, R. F., Burke, K., & Sengor, A. M. C. (1981). Was the Laramide orogeny related to subduction of an oceanic plateau? *Nature (London)*, 289(5795), 276-278.

Merin, I. S., & Lindholm, R. C. (1986). Evidence that the crystalline cores of uplifts adjacent to the Powder River basin were breached during Paleocene time. *The Mountain Geologist*, 23(4), 128-131.

Miller, D. M., Nilsen, T. H., & Bilodeau, W. L. (1992). Late Cretaceous to early Eocene geologic evolution of the U.S. Cordillera. In B. C. Burchfiel, P. W. Lipman & M. L. Zoback (Eds.), *The Cordilleran orogen; conterminous U.S. ()*. United States (USA): Geol. Soc. Am., United States (USA).

Mitra, G., & Frost, B. R. (1981). Mechanisms of deformation within Laramide and preCambrian deformation zones in basement rocks of the Wind River Mountains; Rocky Mountain Foreland Basement Tectonics. *Contributions to Geology*, 19(2), 161-173.

Timmons, J. M., Karlstrom, K. E., Heizler, M. T., & Bowring, S. A. (2001). A synthesis from the Unkar Group of Grand Canyon, and inferences on late Mesoproterozoic intracratonic sedimentation and deformation in the western U.S.; Geological Society of America, Rocky Mountain Section, 53rd annual meeting; Geological Society of America, South-Central Section, 35th annual meeting. Abstracts with Programs - Geological Society of America, 33(5), 20.

Tindall, S. E., & Davis, G. H. (2002). Influence of deformation band shear zones on joint development; Geological Society of America, 2002 annual meeting. Abstracts with Programs - Geological Society of America, 34(6), 372.

Wise, D.U., 2000, Laramide structures in basement and cover of the Beartooth uplift near Red Lodge, Montana: American Association of Petroleum Geologists Bulletin, v.84, no.3, p.360-375.

Yuretich, R.F., Hickey, L.J., & Gregson B.P., 1984, Lacustrine deposits in the Paleocene Fort Union Formation, northern Bighorn Basin, Montana: Journal of Sedimentary Petrology, v.54, no.3, p. 836-852.

Wise, D.U., 1983, Overprinting of Laramide structural grains in the Clark's Fork Canyon area and eastern Beartooth Mountains of Wyoming. Wyoming Geological Association, Annual Field Conference, 34th, Guidebook, P.77-87.